Journal of
Cognitive Neuroscience

Retrieval of sequentially organized episodic events recruits large-scale functional connectivity across the controlled retrieval network

Journal:	*Journal of Cognitive Neuroscience*
Manuscript ID	JOCN-2017-0134
Manuscript Type:	Original
Date Submitted by the Author:	07-Apr-2017
Complete List of Authors:	Nah, Yoonjin; Yonsei University, Department of Psychology; Integrated Neurocognitive Functional Imaging Center, Yonsei University Shin, Na-Young; College of Medicine, The Catholic University of Korea, Department of Radiology; Yonsei University College of Medicine, Department of Radiology; Integrated Neurocognitive Functional Imaging Center, Yonsei University Yi, Sehjung; New York University, Department of Psychology Lee, Seung-Koo; Yonsei University College of Medicine, Department of Radiology; Integrated Neurocognitive Functional Imaging Center, Yonsei University Han, Sanghoon; Yonsei University, Department of Psychology; Integrated Neurocognitive Functional Imaging Center, Yonsei University
Keywords:	Controlled retrieval, Functional connectivity pattern analysis, Sequential episodic memory

Title:

Retrieval of sequentially organized episodic events recruits large-scale functional connectivity across the controlled retrieval network

Authors:

Yoonjin Nah[1,5], Na-Young Shin[2,4,5], Sehjung Yi[3], Seung-Koo Lee[4,5], Sanghoon Han[1,5]

Institutional Affiliations:

[1]Department of Psychology, Yonsei University, Seoul 03722, Korea

[2]Department of Radiology, College of Medicine, The Catholic University of Korea, Seoul 06591, Korea

[3]Department of Psychology, New York University, New York, NY 10003, USA

[4]Department of Radiology, Yonsei University College of Medicine, Seoul 03722, Korea

[5]Integrated Neurocognitive Functional Imaging Center, Yonsei University, Seoul 03722, Korea

Corresponding Authors:

1) Sanghoon Han, Ph.D., Department of Psychology

Yonsei University, Seoul 03722, Korea

Phone: +82-2-2123-5436; Fax: +82-2-2123-8330

Email: sanghoon.han@yonsei.ac.kr

2) Seung-Koo Lee, M.D., Ph.D., Department of Radiology (Co-corresponding Author)

Yonsei University College of Medicine, Seoul 03722, Korea

Phone +82-2-2228-2373; Fax: +82-2-2228-7374

Email: slee@yuhs.ac

Abstract

Temporal information of encoded events allows us to mentally travel to the past, and the ability to remember a series of events is a unique control process in humans. Despite much research on controlled episodic retrieval, little is known about how large-scale connectivity patterns are involved in the retrieval of sequentially organized episodic events. In this study, participants performed two episodic memory tasks in which they were required to recall the encoded items in either the forward or backward direction. Results from univariate functional magnetic resonance imaging (fMRI) analysis indicated that recruitment of the left anterior ventrolateral prefrontal cortex (aVLPFC) increased in the backward retrieval compared to the forward recall conditions. Across a large-scale brain network composed of intrinsically connected brain regions, functional connectivity multivariate pattern analysis (fcMVPA) was used to successfully decode the different sequential retrieval conditions by using the functional connectivity patterns as input data. The results demonstrated that the patterns of interactivity across the brain regions implicated in both controlled retrieval and goal-directed cognitive processes (e.g., lateral and medial prefrontal regions, inferior and superior parietal lobules, middle temporal gyrus, and caudate) were informative in decoding of the sequential retrieval processes. These findings suggest that large-scale networks engage differentially during the sequential retrieval processes of episodic memory.

Keywords:

Controlled retrieval, Functional connectivity pattern analysis, Sequential episodic memory

Episodic memory encompasses vast amounts of information including time, place, and self-referential content, and the memories are tagged to each event allowing the retrieval of past events (see Tulving, 2002 for a review). Of particular importance is the ability to mentally go back and forth in time and re-experience sequential memory events; temporal memory retrieval has been regarded as one of the most uniquely controlled processes in human cognition (Tulving, 1972, 1983). It has been suggested that complex mechanisms, such as executive function, planning, and visuospatial processing, play qualitatively different roles in sequential memory processes (i.e., backward versus forward retrieval) (Lezak, 1995; Schofield & Ashman, 1986). For example, while participants can retrieve a relevant memory target that follows the presented cue item by using the directional flow of encoding context (forward), the reverse may require participants to cognitively travel back from the cue item and search for the target in their long-term memory. Under such circumstances, goal-relevant targets cannot be automatically driven simply by encoding cues; thus, top-down processing such as controlled retrieval is essential for backward retrieval.

Although several laboratory and neuropsychological behavioral studies have shown the presence of backward-retrieval detriment or forward-retrieval advantage mediated by the differential controlled process involved in the different directions of sequential retrieval (Anders & Lillyquist, 1971; Drosopoulos, Windau, Wagner, & Born, 2007; Thomas, Milner, & Haberlandt, 2003), the underlying neural mechanisms involved in the sequential retrieval processes and how each controlled process is differentially recruited in these two directions are yet to be fully discussed. Given that the various cognitive processes mentioned above are involved, it is probable that the most efficient way for the brain to achieve controlled retrieval of sequentially encoded events would be to organize a large-scale network and to interact with other control network regions. However, little research has reported the differential

connectivity patterns that support these processes, especially regarding how large-scale network patterns are recruited for retrieval of temporally organized events.

Previous univariate functional magnetic resonance imaging (fMRI) analyses of blood oxygen level-dependent (BOLD) activity have demonstrated that the left ventrolateral prefrontal cortex (VLPFC), specifically the anterior part (aVLPFC; Brodmann area (BA) 47, the pars orbitalis subarea of the inferior frontal gyrus), play a crucial role in cognitively controlled retrieval processes (see Badre & Wagner, 2007 for a review), such as controlled retrieval of semantic memories (Badre, Poldrack, Pare-Blagoev, Insler, & Wagner, 2005; Han, O'Connor, Eslick, & Dobbins, 2012; Wagner, Pare-Blagoev, Clark, & Poldrack, 2001) and retrieval of contextual information (Dobbins & Han, 2006; Raposo, Han, & Dobbins, 2009). Furthermore, there is increasing evidence that the left aVLPFC intrinsically and functionally couples with other brain regions. For example, Neubert, Mars, Thomas, Sallet, and Rushworth (2014) observed that during the resting-state period, aVLPFC (BA 47) is connected with several brain regions, including other prefrontal sub-areas, the temporal, parietal, and premotor cortices. Similarly, Han et al. (2012) found that the left VLPFC is intrinsically connected with both cortical and subcortical areas, including the bilateral PFC, middle temporal gyrus, parietal, and caudate regions. Recently, functional connectivity findings from task-based fMRI study has also shown similar functional coupling patterns in intrinsically defined networks, such as the inferior parietal, temporal, and striatal regions (Barredo, Oztekin, & Badre, 2015). The results also demonstrated that the left aVLPFC was functionally connected with other large-scale brain networks, such as the frontoparietal control network (Spreng, Stevens, Chamberlain, Gilmore, & Schacter, 2010; Vincent, Kahn, Snyder, Raichle, & Buckner, 2008), which has been suggested to play a crucial role in cognitive control processes (Badre & D'Esposito, 2007; Cabeza, Ciaramelli, Olson, & Moscovitch, 2008; Corbetta, Patel, & Shulman, 2008; Koechlin, Basso, Pietrini, Panzer, &

Grafman, 1999). Taken together, these previous studies collectively raise the possibility that broad, interregional functional connectivity across the brain is involved in the sequential retrieval process, and provide a basis for identifying the relevant node regions in functional connectivity analyses (e.g., aVLPFC, inferior parietal lobule, and striatal regions).

The present fMRI study employed two episodic memory tasks in which participants were presented with a series of word items successively during the encoding run and were then required to retrieve the appropriate words with a directional or temporal distance cue. In this study, we aimed to elucidate the patterns of functional connectivity associated with controlled processes that are implicated in the retrieval of sequentially organized episodic events, either in the forward or backward direction. In addition, we employed a machine learning algorithm (Cortes & Vapnik, 1995; Vapnik, 1999) to assess whether patterns of large-scale whole brain connectivity encompassing the left aVLPFC-seeded intrinsic network can distinguish controlled retrieval processes. In contrast to the bivariate functional connectivity analyses used prevalently in the field, we applied a novel functional connectivity multivariate pattern analysis (fcMVPA) approach with task-dependent time-series extracted in a voxel-wise manner from the whole brain. In addition, to explore the most distinctive network patterns, we employed iterative methods for pattern classification as a function of the number of input features included. This iterative approach has been proven useful in finding the most discriminating patterns for classification of two conditions or groups (Pantazatos, Talati, Pavlidis, & Hirsch, 2012a, 2012b; Pantazatos, Talati, Schneier, & Hirsch, 2014). We hypothesized that sequential retrieval in different directions would demand differential controlled processes based on distinctive networks; thus, the task-based functional connectivity patterns obtained from the sequential retrieval period can be used to distinguish between the forward and backward retrieval processes.

Materials and Methods

Participants

Twenty-two healthy volunteers (8 females; mean age = 23.23, *SD* = 2.39) participated in the experiment and were paid for their time (10,000 South Korean Won/hour). Two participants were excluded from all analyses because of incompletion due to fatigue, and the analysis for the N-back task was conducted with data from only 19 participants because data for one participant were unavailable. All participants had normal or corrected-to-normal vision and were right-handed. Informed consent was obtained in a manner approved by the Institutional Review Board of Yonsei University. Prior to the experiment, participants were screened for any significant medical conditions, including their history of neurological or psychiatric diagnoses.

Experimental Materials and Procedures

The study included three fMRI tasks: two episodic memory tasks (Phases 1 and 2) and one working memory task (N-back) (Fig. 1). Prior to the actual task runs, resting-state data were collected to discover intrinsic functional connectivity. During resting-state data acquisition, participants were instructed to close their eyes while lying awake and to not think of anything in particular or in a systematic way. After resting-state data collection, the actual experimental runs began. Both episodic memory tasks, Phases 1 and 2, consisted of both an encoding and a retrieval runs. The experimental items of the two episodic memory tasks were composed of 90 and 160 common Korean nouns (2 syllable words with 2 Korean letters long) for Phases 1 and 2, respectively. All word items were projected onto a screen with a black background and viewed using a mirror mounted on the head coil. Before starting the actual fMRI scanning experiment runs, participants completed a practice run outside of the scanner using a laptop computer. Both the practice and experimental trials were programmed using

the Cogent 2000 toolbox (www.vislab.ucl.ac.uk/cogent.php) and MATLAB 7.12.0 (The MathWorks, Natick, MA).

---------- Insert Figure 1 about here ----------

During the encoding run of Phase 1, participants were asked to memorize triplets of words (e.g., A–B–C) and each word was presented sequentially for 2 s at the center of the screen. Each trial was followed by an association period for another 8 s, during which the participants were required to mentally make associations with the word triplet. The encoding run included 30 trials for a total of 90 words. In the retrieval run of Phase 1, directional instruction (i.e., forward or backward) for each trial was shown for 2 s, then either the first or last word of a word triplet (A or C) learned in the encoding run was presented as a cue for 2 s. During the next 8 s, participants were required to recall the other two words in sequential order (forward recall; A–B–C) or in the backward direction (backward recall; C–B–A). Finally, participants had another 4 s to choose the correct answer from two options (in forward recall, B–C versus C–B; in backward recall, A–B versus B–A), and the order of the two options was randomized. The retrieval run of Phase 1 consisted of 30 trials of alternating mini-blocks of the forward and backward conditions, and each mini-block included five trials.

Phase 2 was divided into two cycles, and each cycle consisted of both an encoding and a retrieval runs. Therefore, there were two encoding and two retrieval runs in Phase 2: Encoding #1, Retrieval #1, Encoding #2, and Retrieval #2. There was an approximately 2 min interval at the end of each run to provide episodic boundaries between pairs of runs. Each set included a series of five words (e.g., A–B–C–D–E) in the encoding run, and each word was presented sequentially at the center of the screen for 2 s. Rather than an association period used in Phase 1, each set was presented twice in a row. Each run included 16 sets, for a total of 80 words. In the retrieval run, participants were first given 8 s to recall the target word. During this recall period, the third word in each set was presented as a cue, and participants

were then instructed to recall the encoded word that had been presented one or two steps later (forward recall lag-1, lag-2 or D and E, respectively) or earlier (backward recall lag-1, lag-2 or B and A, respectively) according to the directional instruction. The recall period was followed by a recognition test, during which the participants had 4 s to choose the answer between two options that had the same directional context, but different temporal distances (in forward recall, D versus E; in backward recall, A versus B). In contrast to Phase 1, each retrieval condition in Phase 2 had 16 trials, and a total of 64 trials from four conditions were randomly presented.

After completing both Phases 1 and 2, participants performed a working memory task, N-back, during which they were successively presented with a series of single-alphabet letters. The N-back task included a total of three conditions (0-back, 1-back, and 2-back) in a block design. In the 0-back condition, the target was the letter "Z" and participants pressed a button as quickly as possible whenever the letter on the screen matched the target. In the 1-back and 2-back conditions, participants responded if the letter on the screen was identical to the stimulus presented one trial or two trials earlier, respectively. Each condition block consisted of 19 trials and there were four target trials in a block. One cycle was composed of three condition blocks and one mini-resting block, and each cycle was repeated three times in the same order.

fMRI Data Acquisition and Data Analyses

Data Acquisition

Neuroimaging data were acquired with the 3T General Electric Healthcare Discovery MR750 (Waukesha, WI) using an 8-channel radiofrequency head coil. Functional data were obtained with a T2*-weighted gradient-echo echoplanar imaging sequence (TR = 2000 ms, TE = 30 ms, 3.75 × 3.75 × 4.0 mm^3 in-plane resolution, 33 axial slices tilted 30° from the

AC–PC plane to reduce the influence of in-plane susceptibility gradients (Deichmann, Gottfried, Hutton, & Turner, 2003), no gap, and interleaved collection). The first five volumes of each run were discarded prior to the actual data collection to ensure magnetization equilibrium. For Phase 1, 210 and 270 volumes were collected for the encoding and retrieval runs, respectively; in Phase 2, 192 and 224 volumes were collected for the encoding and retrieval runs for each cycle. In addition, 260 volumes were collected for the N-back run. Resting-state MRI data were collected prior to the experimental runs (204 volumes). Participants responded with a magnet-compatible button box placed under the right hand. At the end of the functional imaging runs, 3-dimensional T1-weighted structural images (TR = 8.28 ms, TE = 3.29 ms, FOV = 198 × 220 mm^2, voxel size = 0.77 × 0.86 × 1.0 mm^3, 216 sagittal slices, flip angle = 12°, and no gap) were acquired for visualization.

Functional Data Preprocessing and Analyses

Preprocessing and general linear model (GLM) analyses were conducted using SPM8 (Wellcome Department of Cognitive Neurology, London, U.K.) for all functional data, with the exception of the resting-state data. A slice-timing correction was accomplished by resampling all slices relative to the middle slice. Functional images were then realigned to the first volume for motion correction, spatially normalized to the Montreal Neurological Institute (MNI) template provided with SPM8, then resampled into 3 × 3 × 3 mm^3 size voxels, followed by spatial smoothing using a Gaussian kernel with a full width at a half maximum of 8 mm. We focused on the retrieval runs of Phases 1 and 2 since we were investigating the differences in neural processes between the forward and backward retrieval directions. The GLM analysis for the retrieval run of Phase 1 was modeled using four regressors, forward recall, forward recognition, backward recall, and backward recognition, with durations of 10 s for recall (the cue + recall period) and 4 s for the recognition regressor. Both retrieval runs

of Phase 2 were first concatenated into a single run as Phase 2 was divided into two identical runs. A total of eight regressors (direction type × retrieval type × distance lag; 2 × 2 × 2) were used in GLM modeling: forward recall lag-2, forward recognition lag-2, forward recall lag-1, forward recognition lag-1, backward recall lag-1, backward recognition lag-1, backward recall lag-2, and backward recognition lag-2, with 6 s for recall (2 s after the onset of the cue word) and another 4 s for recognition regressors. One additional nuisance covariate, the run effect regressor, was also modeled which was then regressed out to minimize any effects of concatenating the two retrieval runs. For the N-back analysis, three regressors, each for the 0-back, 1-back, and 2-back conditions, were entered into GLM modeling.

All volumes of each run were treated as temporally correlated time-series and modeled by convolving a canonical hemodynamic response function (HRF) and its temporal derivative (except there was no temporal derivative for N-back due to the block design). The resulting hemodynamic functions were used as covariates in GLM, along with a covariate for the run effect. A high-pass filter (cut off 128 s) was applied to remove low-frequency trends, and an autoregressive AR(1) model + white noise correction was used to estimate and correct for non-sphericity of the error covariance (Friston et al., 2002). The least-square parameter estimates of the best-fitting synthetic HRF for each condition of interest were used in pair-wise contrasts and stored as separate images for each participant; these were then checked against the null hypothesis with one-tailed *t*-tests to determine whether effects of participants were random at the group level. Clusters consisting of five or more contiguous voxels (3 mm isotropic) with $p < .001$ were considered significant.

Resting-State Data Preprocessing and Analysis

Resting-state data were preprocessed using a Data Processing Assistant for Resting-State fMRI (Yan & Zang, 2010) which was developed based on SPM8 and the Resting-State

fMRI Data Analysis Toolkit (Song et al., 2011). For slice-timing correction, realignment, normalization, and smoothing processes of resting-state data, we followed the same protocols as those used for preprocessing of functional data described above. Subsequently, data were detrended and temporally filtered with a low-pass band filter (0.01–0.08 Hz). Furthermore, nuisance covariates including six head motion parameters, global mean signal, white matter signal, and cerebrospinal fluid signal were regressed out to improve the validity of our findings. Seed-to-voxel connectivity maps were generated for each participant using a single seed (i.e., the left aVLPFC) that was functionally defined in the GLM analysis (see Results). A total of 20 connectivity maps were entered into the group level analysis and participants were treated as a random effect to generate node maps to investigate task-dependent connectivity patterns.

Task-Dependent Time-Series and Node Definitions for Connectivity Analysis

To obtain task-dependent time-series reflecting psychological factors, BOLD signal time-series were extracted from the whole brain in a voxel-wise manner for all retrieval runs (270 and 448 TRs in Phases 1 and 2, respectively). The extracted BOLD signal time-series were then deconvolved with a parametric empirical Bayesian formulation to estimate voxel-by-voxel neural time-series, and these were detrended to remove any linear and nonlinear trends. Condition-specific psychological factors were defined by contrasting the onset time points of each recall condition against baseline (i.e., 1 for forward recall conditions and 0 for others during forward retrievals or 1 for backward recall conditions and 0 for others during backward retrievals). Next, condition-weighted time-series were generated separately for the two retrieval directions by multiplying the aforementioned neural time-series with psychological factors. However, since the condition-weighted time-series obtained here were based on neuronal activity, the time-series were convolved again with a canonical HRF to

generate signals that were more closely related to BOLD signals measured with MRI. Finally, HRF-convolved time-series were detrended.

The nodes for additional functional connectivity analyses were defined based on the results of the resting-state analysis. Seed-to-voxel connectivity maps obtained from the resting-state analysis generated 55 peak regions based on SPM-identified whole sub-peak local maxima (see Results). Any peak voxels outside of the gray matter or image boundaries were excluded, which resulted in a total of 35 peak voxels. We then created cube-shaped nodes of 27 voxels (3 × 3 × 3) centered on each peak voxel. To obtain a representative time-series for each node, the first eigenvariate time-series was extracted from whole voxels of the node using the principal component analysis function embedded in MATLAB. This generated a total of 70 task-dependent time-series (35 for forward and 35 for backward retrieval types) for each participant.

Functional Connectivity Multivariate Pattern Analysis

For each participant, pair-wise cross-correlation coefficients (Pearson correlation coefficient) between the time-series of whole nodes were calculated, which generated 35 × 35 symmetrical connectivity matrices, where each element represented a functional connectivity between two nodes. Since the resulting matrices were symmetric with respect to the diagonal, only 595 elements from the lower half of the matrix (i.e., 35 × 34/2) were used as features for further connectivity analyses. For feature selection, 40 iterations of *t*-tests were performed for each feature from two retrieval directions of each participant. Specifically, 39 out of 40 correlation coefficients while putting one sample aside (19 and 20 from forward and backward, respectively, if the selected sample was from the forward type, otherwise 20 forward and 19 backward if the sample was from the backward type) for each iteration were compared to assess the differences between the means of the two populations. Therefore,

each feature had 40 *t*-score values, which were then averaged to generate one representative *t*-score value for the feature. Finally, 595 features were ranked based on the absolute *t*-score values, and z-score transformation was applied to each feature (*r*) to improve normality. To eliminate any directional bias, we used absolute *t*-score values instead of raw values.

To test whether patterns of functional connectivity from each retrieval direction could discriminate between different directions of retrieval processes, we conducted fcMVPA using a linear support vector machine (SVM) algorithm embedded in the Spider v1.71 MATLAB toolbox (http://people.kyb.tuebingen.mpg.de/spider/). For SVM classification, 595 elements of each type that were previously obtained were used as input features, and data from two sets of participants were labeled with two different class labels for tagging the original retrieval direction membership (i.e., 1 and −1 for forward and backward, respectively). Classification accuracies were obtained in succession as a function of a range of included features, which were arranged in descending order by their absolute *t*-score value. Specifically, the N^{th} SVM classification accuracy was obtained using the top N features, for which the *t*-score values were arranged from the highest to N^{th}. Then, the $(N+1)^{th}$ accuracy was calculated by adding an additional feature that had the next highest *t*-score value to the feature that was already included. This process was iterated until the classification used all features, from the top feature to the last feature with the lowest *t*-score value. Therefore, this method resulted in a total of 595 accuracy measures. The purpose of this approach was not to find the algorithm that maximized the prediction accuracy. Instead, it was designed to explore which features were potentially informative in classifying different retrieval types. Furthermore, we investigated the optimal number of features needed for machine learning processes since simply including complete data features for SVM classification may result in noisy information being used to train and test the classifier.

Each SVM classification performance was estimated using a leave-one-out cross validation (LOOCV) procedure. For each iteration of the LOOCV, one sample was removed and the remaining 39 of 40 samples (19 forward and 20 backward types if the selected sample was a forward; alternatively, 20 forward and 19 backward types if the sample was from the backward type) were put into the machine learning algorithm to train the classifier. The excluded sample was then used to test the performance of the classifier: if the classifier predicted the class label of the test sample correctly, accuracy was scored as "1," whereas if an incorrect prediction was made, it was scored as "0." Therefore, there were 40 accuracies estimated from 40 rounds of iterations, which were then averaged to obtain one representative accuracy measure for the N^{th} SVM classification.

To verify that the fcMVPA accuracies were valid, we calculated the null distribution of 1000 permutations. For each permutation testing iteration, a total of 40 original class labels, including 20 class labels "1" and 20 class labels "−1," were randomly shuffled and used for the SVM classification. The classification procedures occurred as conducted with the original data. Representative classification performance was estimated by averaging the results of 1000 iterations. We predicted that if the connectivity patterns of one type (i.e., forward retrieval) were not different from those of the other type (i.e., backward retrieval), the SVM classifier would not be well-trained by the input data and the classification results would thus yield accuracy of approximately 50% (probability of chance). In other words, even if the original class labels of a dataset (i.e., connectivity patterns of certain retrieval directions of one participant) were randomly shuffled while the actual dataset remained unchanged, SVM classification performance would be similar to the results obtained from using true class labels for each retrieval type. In contrast, if connectivity patterns for the two retrieval directions were truly different and if each type had distinctive combinations of connectivity, randomly shuffled class labels for SVM classification should result in an accuracy of

approximately 50%, whereas classification based on the original class labels should yield accuracy above chance.

Results

Behavioral Data

Accuracy (%)

The overall accuracy of the recognition task in Phase 1 was 67%. Participants had better accuracy in the forward condition compared to that in the backward condition (72% versus 62%, respectively; $t(19) = 2.36$, $p = .029$). Overall accuracy of the recognition task in Phase 2 was 71%. Similarly, accuracy in the forward condition was greater than that in the backward condition (76% versus 66%, respectively; $t(19) = 4.57$, $p < .001$) (Fig. 2A). Interestingly, there was a distance effect in the backward condition: the accuracy of the backward lag-2 condition was significantly less than that in the other conditions (backward lag-2 versus backward lag-1, $t(19) = -2.28$, $p = .035$; backward lag-2 versus forward lag-1, $t(19) = -3.27$, $p = .004$; backward lag-2 versus forward lag-2, $t(19) = -5.26$, $p < .001$) (Fig. 2B). There were no differences in accuracy between any load conditions on the N-back task (0-back, $M = 96.49$, $SD = 1.95$; 1-back, $M = 99.12$, $SD = 0.60$; 2-back, $M = 93.86$, $SD = 2.46$), with the exception of marginal differences between 1-back and 2-back conditions ($t(18) = 1.99$, $p = .062$).

---------- Insert Figure 2 about here ----------

Response Time (ms)

The mean response time (RT) on the recognition task in Phase 1 was 2280 ms. RTs in the backward condition were significantly slower than those in the forward condition (2102 ms versus 2458 ms, $t(19) = -4.46$, $p < .001$). Participants also had slower RTs in the backward condition compared to the forward condition in Phase 2 (2017 ms versus 2148 ms, $t(19) = -3.86$, $p = .001$) (Fig. 3A). RTs in both the backward lag-2 and lag-1 conditions in Phase 2 were significantly slower than RTs in the forward lag-1 condition ($t(19) = 2.34$, p

= .031; $t(19) = 4.49$, $p < .001$). There were marginal differences in RTs between the backward lag-1 and forward lag-2 conditions ($t(19) = 1.99$, $p = .061$) (Fig. 3B). Overall RTs in the N-back task averaged 472 ms. The 2-back condition had the slowest RTs, whereas the 1-back condition had the fastest RTs (451 ms, 419 ms, and 544 ms for 0-back, 1-back, and 2-back, respectively; all paired *t*-tests between each condition resulted in statistical differences between the RTs).

---------- Insert Figure 3 about here ----------

Functional Neuroimaging Data

Neural Regions Associated with the Sequential Retrieval Process

To increase the statistical power for detecting brain regions involved in the sequential retrieval process, we used an alternating mini-block design consisting of the forward and backward retrieval conditions in Phase 1. Our aim was to elucidate neural regions associated with the different sequential directions of recall processes; thus, our fMRI analyses mainly focused on the recall periods during each condition. We first calculated the contrast between forward recall versus backward recall, but this analysis did not indicate activation of any brain regions at a significance threshold of $p < .001$. Interestingly, when we contrasted backward recall versus forward recall, we observed activation of the left aVLPFC (BA47), left middle frontal gyrus, left inferior parietal lobule, and left postcentral gyrus (Table 1 and Fig. 4A), indicating that the backward recall condition required additional cognitive demands compared to the forward recall condition.

---------- Insert Figure 4 about here ----------

In Phase 2, we used an event-related design focusing on the recall period again to recapitulate the Phase 1 results and to identify the different neural regions dependent upon directional retrieval during recall processes and on the distance between the cue and the target

(i.e., lag-1 or lag-2). Overall forward versus backward recall contrast (forward lag-1 and lag-2 versus backward lag-1 and lag-2) did not yield any significant activation at a threshold of $p < .001$. In contrast, we found activation of several regions, such as the left aVLPFC, prefrontal, and temporal lobe regions (Table 1 and Fig. 4B), when we used the overall backward versus forward recall contrast. Given these findings from Phases 1 and 2, we concluded that backward retrieval of sequentially organized episodic events was a specific type of controlled retrieval process when compared to forward retrieval and in which the left aVLPFC has been previously implicated to play a role (Badre & Wagner, 2007).

If recruitment of the left aVLPFC resulted from the fact that backward retrieval of episodic events required a more controlled mechanism than forward retrieval, then in Phase 2, we would anticipate that contrasting between the most and the least demanding retrieval control processing conditions would produce similar activation of the left aVLPFC. Therefore, we hypothesized that when participants were cued with the third of five words (cue is the "C" in the list of A–B–C–D–E), retrieval of the first word of the list (i.e., A) would require the most control processes because participants would be required to retrieve stored memories in the backward direction and the target is temporally located at the furthermost end of the word list. In contrast, participants would be expected to retrieve the fourth of five words relatively easily (i.e., D) because it is adjacent to the cue and is located in the forward direction. To examine this hypothesis, we conducted pairwise comparisons between all recall conditions. Our hypothesis was supported by evidence that activation of the left aVLPFC occurred when we used the backward recall lag-2 versus forward recall lag-1 contrast. This demonstrated that manipulation of both the retrieval direction and temporal distance in Phase 2 induced different involvement of control processes. As predicted, no activation of the left aVLPFC was observed when backward recall lag-1 was contrasted with forward recall lag-1 and forward recall lag-2 (Table 1 and Fig. 5).

---------- Insert Figure 5 & Table 1 about here ----------

Consistently, the contrast between backward recall versus forward recall from Phases 1 and 2 indicated activation of the left aVLPFC region. To identify an overlapping cluster in the left aVLPFC and to determine which brain regions were commonly recruited across the phases, we conducted a separate analysis using the backward recall versus forward recall contrast data from Phases 1 and 2. We first relaxed the threshold for both images ($p < .005$) to include more exploratory regions. Two images were then multiplied together, which resulted in overlapping brain regions that were significantly activated in the backward recall versus forward recall across all phases. This analysis yielded an overlapping activation map that included the left aVLPFC, left middle frontal gyrus, and left middle occipital gyrus (Fig. 6A). To ensure that the results obtained from this analysis did not mirror differences in the working memory load required, regions that overlapped with working memory results were excluded by subtracting the contrast results of 2-back versus 0-back (also using a relaxed threshold, $p < .005$) from the overlapping map obtained above (Fig. 6B). Only one region, the left aVLPFC, remained after this analysis was completed, although 3 of 13 voxels in this cluster were also excluded. These results indicated that the left aVLPFC played a crucial role in the controlled retrieval processes that we manipulated in both Phases 1 and 2 (Fig. 6C).

---------- Insert Figure 6 about here ----------

Seed-Based Resting-State Analysis with the Left aVLPFC Cluster

The GLM analyses indicated several brain regions, including the PFC, that were involved in the retrieval processes. These results, however, only indicated differential involvement of the left aVLPFC in sequential retrieval processes, but did not provide information on its interactions with other brain regions. We therefore conducted resting-state intrinsic functional connectivity analysis to elucidate which neural regions were intrinsically connected to the left aVLPFC. The left aVLPFC cluster as indicated by the GLM analyses

was used as the seed region and interactivity (i.e., temporal correlations) of this region with the rest of the brain was assessed in a voxel-wise manner. The results indicated that the aVLPFC was connected to the following regions: the bilateral superior frontal gyri, bilateral middle frontal gyri, bilateral inferior frontal gyri, bilateral medial frontal gyri, bilateral middle temporal gyri, bilateral caudate, left superior parietal lobules, and bilateral inferior parietal lobules (Table 2 and Fig. 7A).

---------- Insert Figure 7 and Table 2 about here ----------

Discriminating between Forward and Backward Retrieval Using Patterns of Functional Connectivity

We generated a left aVLPFC-seeded intrinsic network map using data from the seed-based resting-state connectivity analysis, which was then used to create a total of 35 nodes (See Materials and Methods). To examine how these intrinsically connected brain regions (i.e., 35 nodes, Fig. 7B) interacted with each other during task performance, we conducted fcMVPA using task-based time-series extracted from the retrieval runs of Phases 1 and 2. Specifically, we used fcMVPA to investigate whether forward and backward retrieval processes recruited qualitatively different patterns of functional connectivity. The accuracy results obtained using fcMVPA for Phases 1 and 2 data are shown in Fig. 8. To investigate the number of features (i.e., functional connectivity between two different brain regions) required to produce optimally informative patterns in a classification algorithm, we performed a linear SVM pattern classification which iterated as a function of the number of features included. In Phase 1, SVM classification accuracies were 65% with only one feature and gradually increased to 100% when the top 20 features were included. The classification performance then gradually decreased and reached an accuracy of 43% when the complete set of features was included. The pattern of accuracies in Phase 2 was similar to that in Phase 1, but a greater number of features was required for SVM classification to generate a

maximum classification performance (accuracy of 93% with the top 67 of 595 features), which presumably resulted from the relatively complex experimental task design used in Phase 2.

To test whether the obtained peak accuracies in Phases 1 and 2 were statistically different from the null distribution results, we additionally conducted permutation testing. After 1000 iterations of permutation, we observed that accuracies remained near 50% (Fig. 8). Therefore, we confirmed that the peak accuracies from the original data were derived from distinctive patterns of functional connectivity between the two different retrieval conditions.

---------- Insert Figure 8 about here ----------

We further assessed the critical features included in the peak classification accuracies (100% and 93% in Phases 1 and 2, respectively). In Phase 1, the 20 features included in the peak accuracy were composed of several functional connections among lateral and medial prefrontal regions, supplementary motor area, inferior and superior parietal lobules, middle temporal gyrus, and caudate (Table 3 and Fig. 9A). In Phase 2, a total of 67 features were required to achieve the peak accuracy; the most discriminating patterns of functional connectivity consisted of connections among lateral and medial prefrontal regions, supplementary motor area, inferior and superior parietal lobules, supramarginal gyrus, middle temporal gyrus, and caudate (Table 3 and Fig. 9B). Importantly, in both phases, the patterns of functional connectivity that discriminated between the two different sequential retrieval conditions encompassed regions that have been implicated in cognitive control processes (Badre & D'Esposito, 2007; Cabeza et al., 2008; Corbetta et al., 2008; Koechlin et al., 1999), such as the frontoparietal control network (Spreng et al., 2010; Vincent et al., 2008) and the striatal region (Grahn, Parkinson, & Owen, 2008) related to goal-directed behavior.

---------- Insert Figure 9 & Table 3 about here ----------

Discussion

The aim of the current study was to identify neural regions and to examine patterns of functional connectivity associated with cognitive control processes that were implicated in forward or backward retrieval of sequentially organized episodic events. In the initial univariate analysis, we found that retrieval of episodic events in the backward direction recruited the left aVLPFC more than retrieval in the forward direction. This effect did not merely mirror the different task load between the two sequential retrieval conditions as neural activity in the left aVLPFC was still observed even after subtracting neural activity maps obtained during a separate working memory task. We also noted that patterns of interactivity across a large-scale brain network, comprised of intrinsically connected brain regions with the left aVLPFC based on a bivariate seed-based resting-state connectivity analysis, constructed distinct functional connectivity structures during the two different directional retrieval conditions. Importantly, the multivariate pattern classification analyses using these connectivity patterns as input data reached great accuracy level, demonstrating that task-based interactivity of two sequential retrieval processes recruited qualitatively distinct network patterns. The patterns of functional interactivity across the brain regions implicated in controlled retrieval or goal-directed cognitive process, such as the lateral and medial prefrontal regions, inferior and superior parietal lobules, middle temporal gyrus, and caudate, were informative in decoding the sequential retrieval processes. These findings suggest that the large-scale networks differentially engage in sequential retrieval processes of episodic memory, supporting the proposal that controlled processes are recruited for the retrieval of temporal events and are mirrored in the patterns of functional connectivity.

Recently, functional connectivity analysis has been widely adopted to assess intrinsic or task-related interactivity across distributed brain regions. In contrast to the classical connectivity studies in which only bivariate seed-based connectivity has been applied to the

resting-state scan or psychophysiological interaction (PPI) analysis, to our knowledge, the use of multivariate pattern analysis approach based on the machine learning algorithm using a large-scale functional connectivity matrix as input data has only been adopted in a few studies. For example, studies using task-related fMRI techniques have successfully utilized this approach for decoding neural responses during various cognitive tasks (Pantazatos et al., 2012a, 2012b; Shirer, Ryali, Rykhlevskaia, Menon, & Greicius, 2012). In the present study, we applied the fcMVPA method to decode large-scale neural interactivity underlying controlled retrieval processes. In addition, we did not include all features (i.e., all pair-wise functional connectivity values) into the machine learning process simultaneously. Motivated by recent studies in which a novel fcMVPA approach had been applied (Pantazatos et al., 2012a, 2012b), we instead gradually increased the number of features included with each iteration of SVM classification processes, which resulted in a series of classification accuracies. With this protocol, we could monitor the changes in the pattern of accuracy as a function of the number of features included. As a result, we were able to detect that the usage of 20 features of functional connectivity constructed the most informative patterns in distinguishing between the two different retrieval conditions in Phase 1, whereas 67 features were required to achieve maximum accuracy in Phase 2, which was inherently more complex by design.

Another novel point in our methods was that we extracted more condition-specific time-series instead of simple BOLD time-series for conducting functional connectivity analyses. To achieve this, we first extracted neural time-series across the whole retrieval runs and then convolved them with psychological factors (i.e., two different retrieval directions) to generate condition-weighted time-series in a voxel-by-voxel manner. Convolving neural time-series with psychological factors was originally used for generating interaction terms in the PPI functional connectivity approach (for a review see Friston, 2011; Friston et al., 1997).

In this method, researchers need to define one seed region to examine how other brain regions are functionally coupled with the predefined ROI. This poses a limitation in the number of seed regions, and the results from the PPI analysis represent a relationship only between the seed and other regions and not the interactivity across those regions. In contrast, fcMVPA allows us to examine how each brain region interacts with other areas within a large-scale brain network by simultaneously computing whole pair-wise cross-correlation coefficients.

Previous studies have shown intrinsic functional coupling between the lateral PFC regions and sub-cortical regions such as the caudate (Barnes et al., 2010; Han et al., 2012), and the results from the resting-state functional connectivity analysis in our study corroborate those earlier findings. More importantly, fcMVPA revealed functional coupling between two regions during the task-state period and found that this link played an important role in distinguishing between two retrieval conditions. Specifically, we observed that the right caudate had increased functional connectivity with the left aVLPFC during backward retrieval compared to forward retrieval in Phase 1 (Feature rank #5, $t(19) = 3.03$, $p = .007$), suggesting a possible functional circuit crucial for cognitive control. Given the role of the caudate region in guiding goal-directed behavior (Grahn et al., 2008) and updating working memory (Marklund et al., 2009), we predict that the right caudate will help participants hold the received cue item in the working memory, while the left aVLPFC supports successful backward retrieval in which a controlled retrieval process is required.

During backward retrieval of Phase 1, fcMVPA results also illustrated that the left aVLPFC had stronger functional connectivity with both the right inferior parietal lobule and the right middle frontal gyrus, although the latter did not reach statistical significance (Feature rank #6, $t(19) = 2.96$, $p = .008$; Feature rank #18, $t(19) = 1.90$, $p = .073$). In addition, we found that there was a correlation between the functional connectivity strength of Feature

rank #18 and behavioral performance. Specifically, the difference in correlation coefficients of Feature rank #18 (link between the left aVLPFC and the right middle frontal gyrus #3) between the backward and forward recall conditions was positively correlated with accuracy (%) in the backward recall condition during Phase 1 (r = .48, p = .031; Fig. 10A). It is important to note that these two regions are major components of the frontoparietal network (Spreng et al., 2010; Vincent et al., 2008). Converging neuroimaging evidence suggests that components of the frontoparietal network, including lateral PFC, anterior cingulate cortex, and inferior parietal lobule regions, play a crucial role in cognitive processes in which executive control is required (Badre & D'Esposito, 2007; Cabeza et al., 2008; Corbetta et al., 2008; Koechlin et al., 1999). Therefore, one plausible explanation for the observed functional coupling between the left aVLPFC and the two right nodes in the current study is that the left aVLPFC actively engages in the cognitive control process to access goal-relevant episodic information, while the frontoparietal network supports a more general goal-directed cognitive process.

To identify any underlying traces of the relationships between univariate functional neuroimaging data (i.e., parameter estimate results of the left aVLPFC) and behavioral performances, we conducted an additional correlation analysis. This analysis revealed that there was a positive correlation between the difference in the mean parameter estimate for the left aVLPFC (beta values of the backward recall minus that of the forward recall conditions) and accuracy (%) in the backward recall condition of Phase 1 (r = .45, p = .049; Fig. 10B). We demonstrated that the participants whose left aVLPFC showed disproportionately increased involvement in the backward recall condition compared to the forward recall condition performed better during the backward recall test. The correlation provides some evidence to support the relationship between the role of the left aVLPFC and behavioral performances during the backward retrieval processes, but further research is still needed to

elucidate the exact relationship between neural processes and behavioral outcomes, as our study only showed significant results in Phase 1 and not in Phase 2.

---------- Insert Figure 10 about here ----------

The GLM analyses using the contrast of backward versus forward recall conditions enabled us to observe increased activation of the left aVLPFC. Moreover, this activation did not result from mere differences in the working memory load required between the two conditions, but rather from the demand required for controlled retrieval processes. If retrieval of the studied items backward simply required more working memory load than completing the task in the forward direction, we would expect to observe similar results as those of Sun et al. (2005). In their study, the authors demonstrated that backward recall processes compared to forward recall resulted in higher activity in the dorsolateral PFC (DLPFC, BA9), which indicated that backward recall requires more executive functions (see D'Esposito, Postle, & Rypma, 2000 for a review).

Alternatively, it is also possible that participants retrieve all items from the list (i.e., 3 and 5 words in Phases 1 and 2, respectively) simultaneously, regardless of the directional cue instructions, but then have difficulty selecting the correct answers among the competing alternatives, especially in the backward conditions (Moss et al., 2005; Thompson-Schill, D'Esposito, Aguirre, & Farah, 1997; Thompson-Schill, D'Esposito, & Kan, 1999). In contrast, participants may retrieve the forward target easily but need to actively search their stored memories in the backward conditions to restore their memory representations (Badre et al., 2005; Han et al., 2012; Wagner et al., 2001). If the first hypothesis is correct, we would expect increased activation of mid-VLPFC, which has been implicated in domain-general selection processes that follow retrieval and resolve competition among many retrieved representations. However, if the second explanation was accurate, we would predict that aVLPFC would be activated (see Badre & Wagner, 2007 for a review). Our results are

consistent with this second explanation. Increased involvement of the left aVLPFC during backward retrieval can be explained in terms of controlled retrieval processes.

Although we demonstrated the active involvement of several controlled network regions, it is important to note that informative patterns were not merely composed of connections with either positive or negative correlation coefficients. Importantly, the current findings using multivariate pattern analysis approach suggest that connections with various correlation strengths constructed the most informative patterns in distinguishing between forward and backward sequential retrieval processes, especially in Phase 2. This is consistent with the idea that univariate analysis investigating the amplitude of a single region or bivariate seed-based connectivity analysis may not be adequate to capture the representation or underlying mechanism of complex cognitive processes, especially when the mechanisms involve the interaction of distributed nodes (i.e., Pantazatos et al., 2012a). Nonetheless, the present study shows that the retrieval of sequentially organized episodic events in the backward direction requires increased involvement of the left aVLPFC, in which a controlled retrieval process has been implicated. Moreover, a successful retrieval of sequentially organized episodic events depends upon an interregional interactivity across a large-scale brain network, which has been implicated in goal-directed cognitive process. These patterns of functional connectivity were informative enough in distinguishing the backward retrieval process from the forward retrieval process.

References

Anders, T. R., & Lillyquist, T. D. (1971). Retrieval time in forward and backward recall. *Psychonomic Science, 22*(4), 205-206.

Badre, D., & D'Esposito, M. (2007). Functional magnetic resonance imaging evidence for a hierarchical organization of the prefrontal cortex. *Journal of Cognitive Neuroscience, 19*(12), 2082-2099.

Badre, D., Poldrack, R. A., Pare-Blagoev, E. J., Insler, R. Z., & Wagner, A. D. (2005). Dissociable controlled retrieval and generalized selection mechanisms in ventrolateral prefrontal cortex. *Neuron, 47*(6), 907-918.

Badre, D., & Wagner, A. D. (2007). Left ventrolateral prefrontal cortex and the cognitive control of memory. *Neuropsychologia, 45*(13), 2883-2901.

Barnes, K. A., Cohen, A. L., Power, J. D., Nelson, S. M., Dosenbach, Y. B., Miezin, F. M., et al. (2010). Identifying basal ganglia divisions in individuals using resting-state functional connectivity MRI. *Frontiers in Systems Neuroscience, 4*, 18.

Barredo, J., Oztekin, I., & Badre, D. (2015). Ventral fronto-temporal pathway supporting cognitive control of episodic memory retrieval. *Cerebral Cortex, 25*(4), 1004-1019.

Cabeza, R., Ciaramelli, E., Olson, I. R., & Moscovitch, M. (2008). The parietal cortex and episodic memory: an attentional account. *Nature Reviews Neuroscience, 9*(8), 613-625.

Corbetta, M., Patel, G., & Shulman, G. L. (2008). The reorienting system of the human brain: from environment to theory of mind. *Neuron, 58*(3), 306-324.

Cortes, C., & Vapnik, V. N. (1995). Support-vector networks. *Machine Learning, 20*(3), 273-297.

D'Esposito, M., Postle, B. R., & Rypma, B. (2000). Prefrontal cortical contributions to working memory: evidence from event-related fMRI studies. *Experimental Brain Research, 133*(1), 3-11.

Deichmann, R., Gottfried, J. A., Hutton, C., & Turner, R. (2003). Optimized EPI for fMRI studies of the orbitofrontal cortex. *Neuroimage, 19*(2), 430-441.

Dobbins, I. G., & Han, S. (2006). Cue- versus probe-dependent prefrontal cortex activity during contextual remembering. *Journal of Cognitive Neuroscience, 18*(9), 1439-1452.

Drosopoulos, S., Windau, E., Wagner, U., & Born, J. (2007). Sleep enforces the temporal order in memory. *PLoS One, 2*(4), e376.

Friston, K. J. (2011). Functional and effective connectivity: a review. *Brain Connect, 1*(1), 13-36.

Friston, K. J., Buechel, C., Fink, G. R., Morris, J., Rolls, E., & Dolan, R. J. (1997). Psychophysiological and modulatory interactions in neuroimaging. *Neuroimage, 6*(3), 218-229.

Friston, K. J., Glaser, D. E., Henson, R. N., Kiebel, S., Phillips, C., & Ashburner, J. (2002). Classical and Bayesian inference in neuroimaging: applications. *Neuroimage, 16*(2), 484-512.

Grahn, J. A., Parkinson, J. A., & Owen, A. M. (2008). The cognitive functions of the caudate nucleus. *Progress in Neurobiology, 86*(3), 141-155.

Han, S., O'Connor, A. R., Eslick, A. N., & Dobbins, I. G. (2012). The role of left ventrolateral prefrontal cortex during episodic decisions: semantic elaboration or resolution of episodic interference? *Journal of Cognitive Neuroscience, 24*(1), 223-234.

Koechlin, E., Basso, G., Pietrini, P., Panzer, S., & Grafman, J. (1999). The role of the anterior prefrontal cortex in human cognition. *Nature, 399*(6732), 148-151.

Lezak, M. D. (1995). *Neuropsychological assessment*. New York: Oxford University Press.

Marklund, P., Larsson, A., Elgh, E., Linder, J., Riklund, K. A., Forsgren, L., et al. (2009). Temporal dynamics of basal ganglia under-recruitment in Parkinson's disease: transient caudate abnormalities during updating of working memory. *Brain, 132*, 336-346.

Moss, H. E., Abdallah, S., Fletcher, P., Bright, P., Pilgrim, L., Acres, K., et al. (2005). Selecting among competing alternatives: selection and retrieval in the left inferior frontal gyrus. *Cerebral Cortex, 15*(11), 1723-1735.

Neubert, F. X., Mars, R. B., Thomas, A. G., Sallet, J., & Rushworth, M. F. (2014). Comparison of human ventral frontal cortex areas for cognitive control and language with areas in monkey frontal cortex. *Neuron, 81*(3), 700-713.

Pantazatos, S. P., Talati, A., Pavlidis, P., & Hirsch, J. (2012a). Cortical functional connectivity decodes subconscious, task-irrelevant threat-related emotion processing. *Neuroimage, 61*(4), 1355-1363.

Pantazatos, S. P., Talati, A., Pavlidis, P., & Hirsch, J. (2012b). Decoding unattended fearful faces with whole-brain correlations: an approach to identify condition-dependent large-scale functional connectivity. *PLoS Computational Biology, 8*(3), e1002441.

Pantazatos, S. P., Talati, A., Schneier, F. R., & Hirsch, J. (2014). Reduced anterior temporal and hippocampal functional connectivity during face processing discriminates individuals with social anxiety disorder from healthy controls and panic disorder, and increases following treatment. *Neuropsychopharmacology, 39*(2), 425-434.

Raposo, A., Han, S., & Dobbins, I. G. (2009). Ventrolateral prefrontal cortex and self-initiated semantic elaboration during memory retrieval. *Neuropsychologia, 47*(11), 2261-2271.

Schofield, N. J., & Ashman, A. F. (1986). The relationship between digit span and cognitive processing across ability groups. *Intelligence, 10*(1), 59-73.

Shirer, W. R., Ryali, S., Rykhlevskaia, E., Menon, V., & Greicius, M. D. (2012). Decoding subject-driven cognitive states with whole-brain connectivity patterns. *Cerebral Cortex, 22*(1), 158-165.

Song, X. W., Dong, Z. Y., Long, X. Y., Li, S. F., Zuo, X. N., Zhu, C. Z., et al. (2011). REST: a toolkit for resting-state functional magnetic resonance imaging data processing. *PLoS One, 6*(9), e25031.

Spreng, R. N., Stevens, W. D., Chamberlain, J. P., Gilmore, A. W., & Schacter, D. L. (2010). Default network activity, coupled with the frontoparietal control network, supports goal-directed cognition. *Neuroimage, 53*(1), 303-317.

Sun, X., Zhang, X., Chen, X., Zhang, P., Bao, M., Zhang, D., et al. (2005). Age-dependent brain activation during forward and backward digit recall revealed by fMRI. *Neuroimage, 26*(1), 36-47.

Thomas, J. G., Milner, H. R., & Haberlandt, K. F. (2003). Forward and backward recall: different response time patterns, same retrieval order. *Psychological Science, 14*(2), 169-174.

Thompson-Schill, S. L., D'Esposito, M., Aguirre, G. K., & Farah, M. J. (1997). Role of left inferior prefrontal cortex in retrieval of semantic knowledge: a reevaluation. *Proceedings of the National Academy of Sciences, U.S.A., 94*(26), 14792-14797.

Thompson-Schill, S. L., D'Esposito, M., & Kan, I. P. (1999). Effects of repetition and competition on activity in left prefrontal cortex during word generation. *Neuron, 23*(3), 513-522.

Tulving, E. (1972). Episodic and semantic memory. In E. Tulving & W. Donaldson (Eds.), *Organization of memory* (pp. 381-403). New York: Academic Press.

Tulving, E. (1983). *Elements of episodic memory*. Oxford: Clarendon Press.

Tulving, E. (2002). Episodic memory: from mind to brain. *Annual Review of Psychology, 53*, 1-25.

Vapnik, V. N. (1999). An overview of statistical learning theory. *IEEE Transactions on Neural Networks, 10*(5), 988-999.

Vincent, J. L., Kahn, I., Snyder, A. Z., Raichle, M. E., & Buckner, R. L. (2008). Evidence for a frontoparietal control system revealed by intrinsic functional connectivity. *Journal of Neurophysiology, 100*(6), 3328-3342.

Wagner, A. D., Pare-Blagoev, E. J., Clark, J., & Poldrack, R. A. (2001). Recovering meaning: left prefrontal cortex guides controlled semantic retrieval. *Neuron, 31*(2), 329-338.

Yan, C. G., & Zang, Y. F. (2010). DPARSF: a MATLAB toolbox for "pipeline" data analysis of resting-state fMRI. *Frontiers in Systems Neuroscience, 4*, 13.

Tables

Table 1. Whole brain GLM analyses. Results of the retrieval runs from Phases 1 and 2.

Regions	Hemisphere	BA	MNI Coordinates			*t*-score
			x	y	z	
Phase 1,						
Backward recall vs. Forward recall						
Inferior Frontal Gyrus	L	47	−48	39	−9	4.57
Middle Frontal Gyrus	L	6	−30	−9	66	4.72
	L	6	−39	6	63	4.04
Inferior Parietal Lobule	L	40	−39	−45	51	4.67
Postcentral Gyrus	L	3	−51	−18	60	3.96
	L	2	−57	−30	48	3.81
	L	2	−54	−30	57	3.81
Phase 2,						
Backward recall vs. Forward recall						
Inferior/Middle Frontal Gyrus	L	47/11	−30	45	−9	4.62
Superior Frontal Gyrus	L	8	−12	33	63	5.47
Middle Frontal Gyrus	R	8	33	27	57	4.44
	L	9	−45	21	48	4.35
	L	6	−42	3	48	4.15
	L	44	−51	21	42	4.10
	R	9	33	12	48	3.79
Medial Frontal Gyrus	R	8	6	27	54	4.01
Supplementary Motor Area	L	8	−9	24	51	4.70
Middle Temporal Gyrus	L	20	−57	−30	−18	4.44
Inferior Temporal Gyrus	L	20	−51	−21	−27	4.15
	L	20	−51	−9	−30	3.75
Superior Occipital Gyrus	L	19	−27	−84	39	4.57
Cuneus	R	18	3	−78	33	3.79

Backward recall lag-2 vs.						
Forward recall lag-1 (Phase 2)						
Inferior Frontal Gyrus	L	47	−33	45	−9	4.41
Superior Frontal Gyrus	L	10	−21	60	12	4.72
Middle Frontal Gyrus	R	10	33	60	6	5.36
	R	9	36	27	57	4.84
	R	9	33	15	48	4.30
	L	8	−36	9	60	4.24
Inferior Temporal Gyrus	L	20	−48	−24	−24	5.59
	L	20	−57	−24	−24	5.34
	L	20	−54	−33	−18	5.15
	R	20	57	−24	−21	4.58
	R	20	57	−18	−27	4.50
	R	20	45	−6	−27	3.96
Angular Gyrus	L	39	−45	−72	36	4.74
Precuneus	R	7	3	−72	36	3.69
Superior Occipital Gyrus	L	19	−27	−84	42	4.54
Calcarine	L	17	−24	−51	12	3.78
Backward recall lag-1 vs.						
Forward recall lag-1 (Phase 2)						
Superior Frontal Gyrus	L	9	−9	48	54	5.08
Angular Gyrus	L	39	−48	−75	33	3.75
Backward recall lag-1 vs.						
Forward recall lag-2 (Phase 2)						
Superior Frontal Gyrus	L	8	−9	33	63	4.61
	R	8	3	27	54	3.96
Supplementary Motor Area	L	8	−6	24	51	3.71

Table 2. Seed-based resting-state analysis. The left aVLPFC cluster was used as the seed region.

Regions	Hemisphere	BA	MNI Coordinates			*t*-score
			x	y	z	
Seed-based						
Resting-state Analysis						
Inferior Frontal Gyrus*	L	47	−42	42	−12	42.22
*(Left anterior VLPFC, seed region)						
Superior Frontal Gyrus	L	8	−15	30	60	6.39
	R	9	9	42	57	6.38
	R	8	6	30	57	6.28
Middle Frontal Gyrus	L	8	−30	15	54	11.37
	L	44	−42	12	36	10.56
	L	44	−48	21	33	10.55
	R	48	48	21	30	6.82
	R	45	57	27	30	6.70
	R	45	51	33	24	6.54
	R	44	54	24	39	6.38
	R	11	24	48	−9	5.33
	R	9	42	18	57	4.27
Inferior Frontal Gyrus	L	48	−54	15	12	10.36
	L	45	−48	27	6	10.20
	L	45	−45	24	15	9.13
	R	47	42	42	−12	13.78
	R	45	51	27	3	7.49
	R	45	45	24	12	5.73
	R	45	60	24	18	4.42
Medial Frontal Gyrus	L	8	−6	36	42	7.05
	R	9	3	48	51	5.21
Supplementary Motor Area	L	8	−6	21	51	9.19
Middle Temporal Gyrus	L	20	−60	−45	−12	8.24
	L	21	−51	−51	9	4.71

	R	20	60	−30	−15	7.44
Caudate	L	N/A	−9	0	18	6.41
	L	25	−12	12	6	6.30
	R	25	9	15	3	4.86
	R	N/A	12	3	18	4.76
Superior Parietal Lobule	L	7	−36	−72	51	9.93
Inferior Parietal Lobule	L	40	−51	−57	51	13.89
	R	39	48	−63	54	7.85
	R	40	60	−48	48	6.99
Supramarginal Gyrus	L	39	−42	−51	33	10.54
Cerebellum	R	N/A	24	−84	−48	9.07
	R	N/A	42	−78	−48	7.76
	R	N/A	21	−69	−36	6.43
	R	N/A	12	−84	−27	5.03
	L	N/A	−36	−72	−45	6.07
	L	N/A	−30	−87	−48	4.15
	L	N/A	−12	−87	−30	5.16

Table 3. Features that were included (edges between the two nodes) for peak accuracies. Peak accuracies of 100% and 93% were achieved in Phases 1 and 2, respectively.

Feature rank	Edge (Node #1–Node #2)	Mean *r*-value		*p*-value
		FR	BR	
	Phase 1			
1	Caudate_L_#1–Middle_Frontal_Gyrus_R_#1	−.07	.19	.002
2	Caudate_R_#1–Middle_Frontal_Gyrus_R_#1	−.08	.24	.003
3	Caudate_R_#1–Inferior_Frontal_Gyrus_R_#3	−.05	.28	.003
4	Middle_Frontal_Gyrus_L_#3–Middle_Frontal_Gyrus_R_#2	.40	−.07	.003
5	Caudate_R_#1–Inferior_Frontal_Gyrus_L_#1	−.004	.25	.003
6	Inferior_Parietal_Lobule_R_#1–Inferior_Frontal_Gyrus_L_#1	−.11	.14	.004
7	Supplementary_Motor_Area_L–Middle_Frontal_Gyrus_R_#2	.36	−.10	.006
8	Superior_Frontal_Gyrus_R_#1–Medial_Frontal_Gyrus_R	.44	−.10	.008
9	Middle_Frontal_Gyrus_R_#4–Superior_Frontal_Gyrus_R_#2	−.09	.25	.012
10	Middle_Frontal_Gyrus_R_#5–Superior_Frontal_Gyrus_R_#2	.07	.33	.015
11	Middle_Temporal_Gyrus_L_#2–Middle_Frontal_Gyrus_R_#2	.25	−.02	.021
12	Superior_Parietal_Lobule_L–Inferior_Frontal_Gyrus_L_#2	.20	−.08	.024
13	Superior_Parietal_Lobule_L–Medial_Frontal_Gyrus_R	.22	−.11	.024
14	Superior_Frontal_Gyrus_L–Middle_Frontal_Gyrus_R_#1	.01	.20	.029
15	Superior_Parietal_Lobule_L–Caudate_L_#1	−.09	.10	.032
16	Superior_Parietal_Lobule_L–Middle_Frontal_Gyrus_L_#1	.37	.03	.036
17	Caudate_L_#1–Middle_Frontal_Gyrus_R_#3	−.08	.21	.036
18	Middle_Frontal_Gyrus_R_#3–Inferior_Frontal_Gyrus_L_#1	.05	.25	.038
19	Middle_Temporal_Gyrus_L_#2–Inferior_Frontal_Gyrus_L_#2	.06	.21	.040
20	Caudate_L_#1–Inferior_Frontal_Gyrus_R_#4	−.10	.09	.041
	Phase 2			

1	Middle_Frontal_Gyrus_L_#1–Superior_Frontal_Gyrus_L	.28	−.04	.006
2	Middle_Temporal_Gyrus_L_#1–Superior_Frontal_Gyrus_L	.11	−.10	.007
3	Inferior_Parietal_Lobule_R_#2–Inferior_Frontal_Gyrus_R_#2	.19	−.11	.008
4	Superior_Parietal_Lobule_L–Superior_Frontal_Gyrus_L	.21	−.18	.009
5	Middle_Frontal_Gyrus_R_#6–Inferior_Frontal_Gyrus_R_#4	.22	−.04	.012
6	Caudate_L_#1–Inferior_Frontal_Gyrus_L_#2	−.10	.15	.014
7	Middle_Temporal_Gyrus_R–Inferior_Frontal_Gyrus_R_#4	.24	−.02	.015
8	Inferior_Parietal_Lobule_R_#2–Caudate_R_#1	.22	−.000 2	.015
9	Middle_Frontal_Gyrus_L_#2–Inferior_Frontal_Gyrus_R_#1	−.04	.18	.019
10	Middle_Temporal_Gyrus_R–Supplementary_Motor_Area_L	.13	−.05	.024
11	Middle_Frontal_Gyrus_L_#3–Superior_Frontal_Gyrus_R_#2	.19	−.01	.025
12	Middle_Frontal_Gyrus_L_#3–Caudate_R_#1	.22	−.01	.026
13	Middle_Temporal_Gyrus_R–Caudate_R_#1	.17	−.02	.030
14	Caudate_R_#2–Superior_Frontal_Gyrus_R_#2	−.03	.17	.035
15	Superior_Parietal_Lobule_L–Medial_Frontal_Gyrus_R	−.15	.14	.045
16	Middle_Frontal_Gyrus_R_#3–Middle_Frontal_Gyrus_R_#2	.10	.51	.047
17	Caudate_R_#2–Inferior_Frontal_Gyrus_R_#3	.17	−.04	.049
18	Middle_Frontal_Gyrus_L_#3–Medial_Frontal_Gyrus_L	.32	.04	.050
19	Caudate_R_#2–Middle_Frontal_Gyrus_L_#1	.14	−.05	.053
20	Inferior_Parietal_Lobule_R_#2–Supplementary_Motor_Area_L	.32	.06	.059
21	Supplementary_Motor_Area_L–Superior_Frontal_Gyrus_R_#1	.13	−.05	.059
22	Superior_Parietal_Lobule_L–Inferior_Parietal_Lobule_R_#1	−.07	.22	.062
23	Middle_Temporal_Gyrus_R–Superior_Frontal_Gyrus_R_#1	.25	.06	.064
24	Supramarginal_Gyrus_L–Inferior_Frontal_Gyrus_L_#3	.05	.28	.065
25	Inferior_Frontal_Gyrus_R_#4–Inferior_Frontal_Gyrus_R_#3	.31	−.02	.066

26	Caudate_R_#1–Inferior_Frontal_Gyrus_L_#2	−.03	.16	.068
27	Supplementary_Motor_Area_L–Middle_Frontal_Gyrus_R_#4	.39	.12	.071
28	Caudate_L_#1–Supplementary_Motor_Area_L	−.02	.21	.073
29	Superior_Frontal_Gyrus_R_#2–Inferior_Frontal_Gyrus_L_#1	−.01	.14	.073
30	Caudate_R_#1–Inferior_Frontal_Gyrus_R_#3	.27	.09	.076
31	Caudate_R_#1–Supplementary_Motor_Area_L	.29	.07	.077
32	Middle_Frontal_Gyrus_R_#4–Inferior_Frontal_Gyrus_R_#3	.36	.08	.079
33	Supplementary_Motor_Area_L–Inferior_Frontal_Gyrus_R_#5	.22	−.01	.080
34	Inferior_Parietal_Lobule_R_#2–Middle_Temporal_Gyrus_L_#1	.14	−.02	.083
35	Caudate_L_#1–Middle_Frontal_Gyrus_R_#3	−.06	.14	.086
36	Middle_Frontal_Gyrus_R_#4–Inferior_Frontal_Gyrus_L_#1	.21	.02	.091
37	Middle_Frontal_Gyrus_R_#5–Middle_Frontal_Gyrus_R_#4	.39	.11	.092
38	Superior_Frontal_Gyrus_R_#2–Superior_Frontal_Gyrus_R_#1	.46	.10	.096
39	Inferior_Parietal_Lobule_L–Middle_Frontal_Gyrus_R_#2	−.01	.25	.098
40	Middle_Temporal_Gyrus_L_#1–Superior_Frontal_Gyrus_R_#1	.14	−.01	.100
41	Middle_Frontal_Gyrus_R_#2~ Medial_Frontal_Gyrus_L	.16	.38	.102
42	Inferior_Parietal_Lobule_R_#2–Middle_Frontal_Gyrus_R_#3	.27	.01	.102
43	Inferior_Frontal_Gyrus_L_#3–Superior_Frontal_Gyrus_L	.21	.05	.103
44	Caudate_L_#1–Medial_Frontal_Gyrus_L	−.04	.15	.103
45	Inferior_Parietal_Lobule_R_#2–Caudate_L_#1	−.05	.12	.104
46	Caudate_R_#2–Middle_Frontal_Gyrus_L_#2	.04	.17	.110
47	Caudate_R_#1–Medial_Frontal_Gyrus_L	.22	.03	.113
48	Inferior_Frontal_Gyrus_L_#4–Caudate_R_#1	.18	.02	.117
49	Middle_Temporal_Gyrus_R–Inferior_Frontal_Gyrus_R_#1	.18	.02	.117
50	Medial_Frontal_Gyrus_R–Middle_Frontal_Gyrus_R_#1	.02	.18	.118
51	Inferior_Frontal_Gyrus_L_#3–Middle_Frontal_Gyrus_R_#1	.14	.003	.122

52	Middle_Frontal_Gyrus_R_#6–Superior_Frontal_Gyrus_L	−.03	.22	.124
53	Caudate_R_#1–Inferior_Frontal_Gyrus_R_#4	.23	.09	.124
54	Middle_Temporal_Gyrus_L_#2–Inferior_Frontal_Gyrus_R_#3	.13	−.06	.125
55	Middle_Temporal_Gyrus_L_#1–Caudate_R_#1	.16	.05	.126
56	Caudate_L_#2–Inferior_Frontal_Gyrus_R_#2	.12	.02	.128
57	Caudate_L_#1–Middle_Frontal_Gyrus_R_#1	−.001	.15	.128
58	Middle_Frontal_Gyrus_R_#4–Middle_Frontal_Gyrus_R_#1	.11	−.08	.130
59	Inferior_Parietal_Lobule_R_#2–Superior_Frontal_Gyrus_R_#2	.26	.05	.131
60	Middle_Frontal_Gyrus_L_#3–Inferior_Frontal_Gyrus_R_#1	.05	.18	.136
61	Middle_Frontal_Gyrus_L_#2–Middle_Frontal_Gyrus_R_#4	−.02	.16	.138
62	Inferior_Parietal_Lobule_R_#2–Superior_Frontal_Gyrus_L	.16	−.04	.140
63	Supramarginal_Gyrus_L–Middle_Frontal_Gyrus_R_#3	.04	.22	.141
64	Middle_Frontal_Gyrus_R_#6–Middle_Frontal_Gyrus_R_#4	.08	.33	.142
65	Inferior_Frontal_Gyrus_R_#3–Superior_Frontal_Gyrus_R_#1	.20	.04	.142
66	Inferior_Frontal_Gyrus_R_#3–Medial_Frontal_Gyrus_R	.17	.02	.144
67	Middle_Temporal_Gyrus_R–Middle_Frontal_Gyrus_R_#5	.11	−.02	.144

Abbreviations: FR, forward retrieval; BR, backward retrieval; R, right hemisphere; L, left hemisphere.

Figure Captions

Figure 1. Schematic figure of the experimental paradigm and stimuli examples. (A) A series of word triplets were successively presented during the encoding run of Phase 1. The retrieval run consisted of two different conditions. Participants were required to retrieve the other two words in sequential order in the forward or backward direction. (B) A series of five words was presented during the encoding run of Phase 2. Participants were asked to remember the target word presented one or two steps later or earlier in the forward or backward condition, respectively. (C) The N-back working memory task consisted of three different conditions (i.e., 0-back, 1-back, and 2-back) in a block design, followed by a mini-resting block.

Figure 2. Behavioral results of the mean accuracy. (A) Mean accuracy in Phases 1 and 2. (B) Results from four different conditions in Phase 2. Error bars represent standard errors of the mean. ***$p < .001$, **$p < .01$, *$p < .05$.

Figure 3. Behavioral results of the mean response time (RT). (A) Mean RTs in Phases 1 and 2. (B) Results from four different conditions in Phase 2. Error bars represent standard errors of the mean. ***$p < .001$, **$p < .01$, *$p < .05$.

Figure 4. General linear model analysis results. (A) Contrast results for backward versus forward recall conditions in Phase 1. (B) Results from identical contrasts (backward > forward recall conditions) in Phase 2.

Figure 5. General linear model analysis results of different lag distances. Contrast results for backward versus forward recall conditions with different lag distances in Phase 2.

(A) Backward lag-2 > forward lag-1. (B) Backward lag-1 > forward lag-1. (C) Backward lag-1 > forward lag-2.

Figure 6. Brain regions commonly recruited across the phases. (A) Overlapping activation map based on the backward versus forward recall results (threshold, $p < .005$) from Phases 1 and 2. (B) Contrast results (threshold, $p < .005$) of 2-back versus 0-back conditions on the N-back task. (C) Subtracting contrast results of the N-back working memory from the overlapping activation map (i.e., A–B) yielded a single cluster ROI in the left anterior ventrolateral prefrontal cortex (aVLPFC).

Figure 7. Seed-based resting-state analysis results. (A) Seed-based resting-state analysis, with the left anterior ventrolateral prefrontal cortex (aVLPFC) cluster as the seed region. (B) A total of 35 nodes (shown in red dots) obtained from the seed-based resting-state analysis. Each cube-shaped node was composed of 27 voxels centered on each peak voxel. Plotted nodes are spherical for visualization purposes. From top left in a clockwise direction: sagittal (left lateral), axial (top), sagittal (right lateral), coronal (back), axial (bottom), and coronal (front) views.

Figure 8. Classification results for functional connectivity multivariate pattern analysis. The thick black lines represent the discrimination accuracies of the support vector machine (SVM) classifier (backward vs. forward retrieval) as a function of the range of features included. Peak accuracies of 100% (Phase 1, A) and 93% (Phase 2, B) were obtained when 20 and 67 features were included in the classification, respectively. The thin black dashed line represents the results of permutation testing, and error bars indicate standard deviation.

Figure 9. Visualization of included features (edges between the two nodes shown in black lines) and nodes (shown in red dots) at the peak accuracies (100% and 93%, Phases 1 and 2, respectively). A total of 20 features and 21 nodes from Phase 1 (A) and 67 features and 35 nodes from Phase 2 (B) are plotted on the brain template. From top left in a clockwise direction for both panels: sagittal (left lateral), axial (top), sagittal (right lateral), coronal (back), axial (bottom), and coronal (front) views.

Figure 10. Results of the correlation analysis. (A) The difference in correlation coefficients of the Feature rank #18 (link between the left anterior ventrolateral prefrontal cortex (aVLPFC)–right middle frontal gyrus #3) between two recall conditions (backward recall minus forward recall) was positively correlated with accuracy (%) in the backward condition in Phase 1. (B) A significant positive correlation was observed between the difference in mean parameter estimate for the left aVLPFC (beta values of backward recall minus that of forward recall conditions) and accuracy (%) in the backward condition in Phase 1.

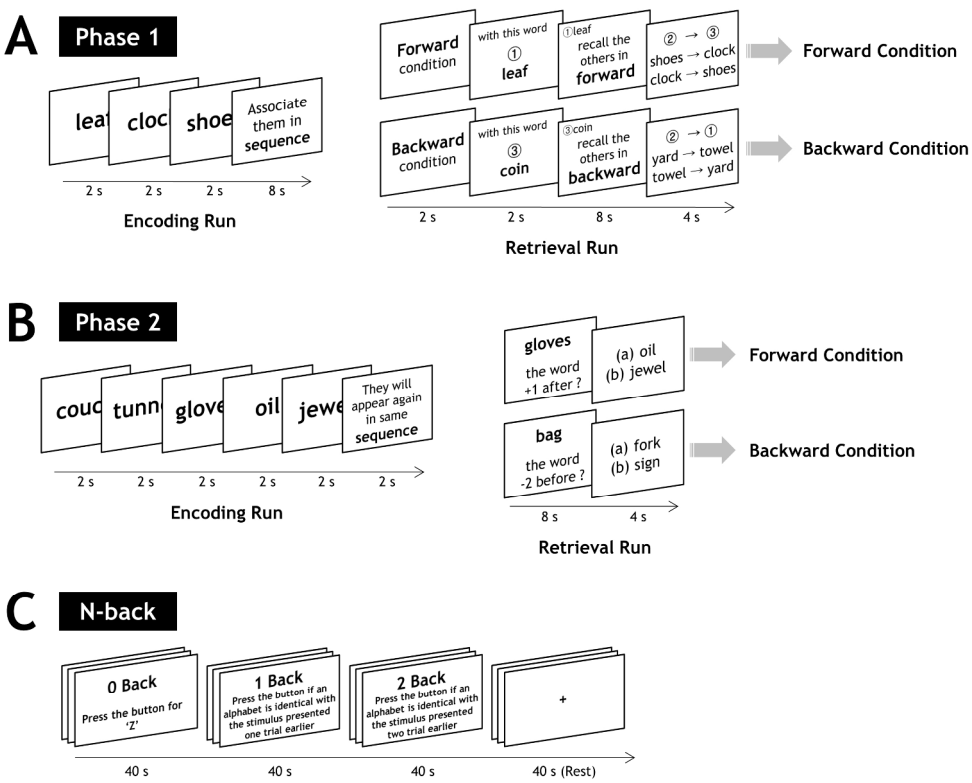

Figure 1. Schematic figure of the experimental paradigm and stimuli examples. (A) A series of word triplets were successively presented during the encoding run of Phase 1. The retrieval run consisted of two different conditions. Participants were required to retrieve the other two words in sequential order in the forward or backward direction. (B) A series of five words was presented during the encoding run of Phase 2. Participants were asked to remember the target word presented one or two steps later or earlier in the forward or backward condition, respectively. (C) The N-back working memory task consisted of three different conditions (i.e., 0-back, 1-back, and 2-back) in a block design, followed by a mini-resting block.

238x187mm (300 x 300 DPI)

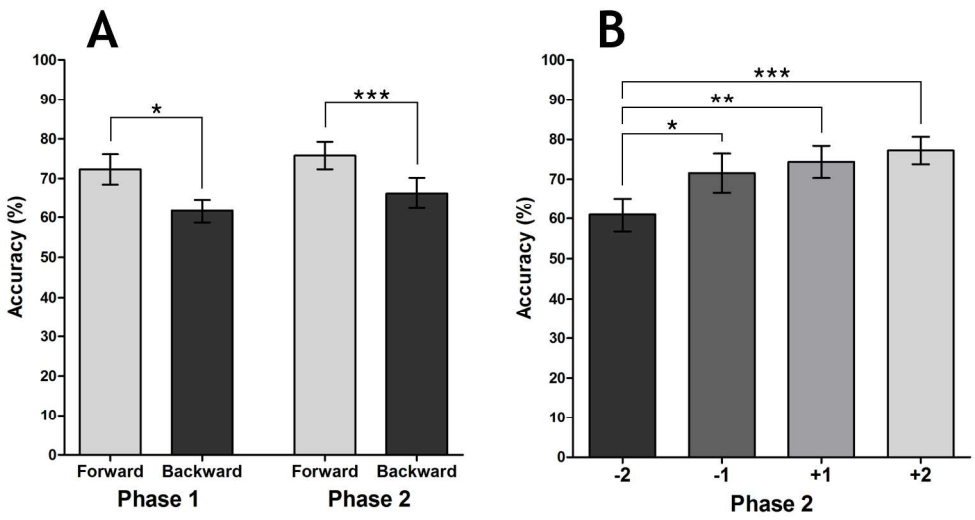

Figure 2. Behavioral results of the mean accuracy. (A) Mean accuracy in Phases 1 and 2. (B) Results from four different conditions in Phase 2. Error bars represent standard errors of the mean. ***p < .001, **p < .01, *p < .05.

250x133mm (300 x 300 DPI)

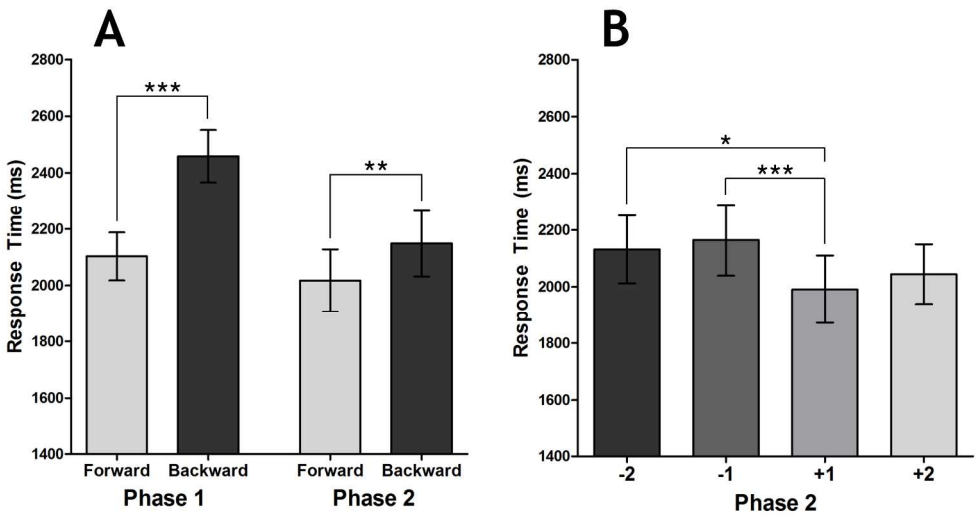

Figure 3. Behavioral results of the mean response time (RT). (A) Mean RTs in Phases 1 and 2. (B) Results from four different conditions in Phase 2. Error bars represent standard errors of the mean. ***p < .001, **p < .01, *p < .05.

251x132mm (300 x 300 DPI)

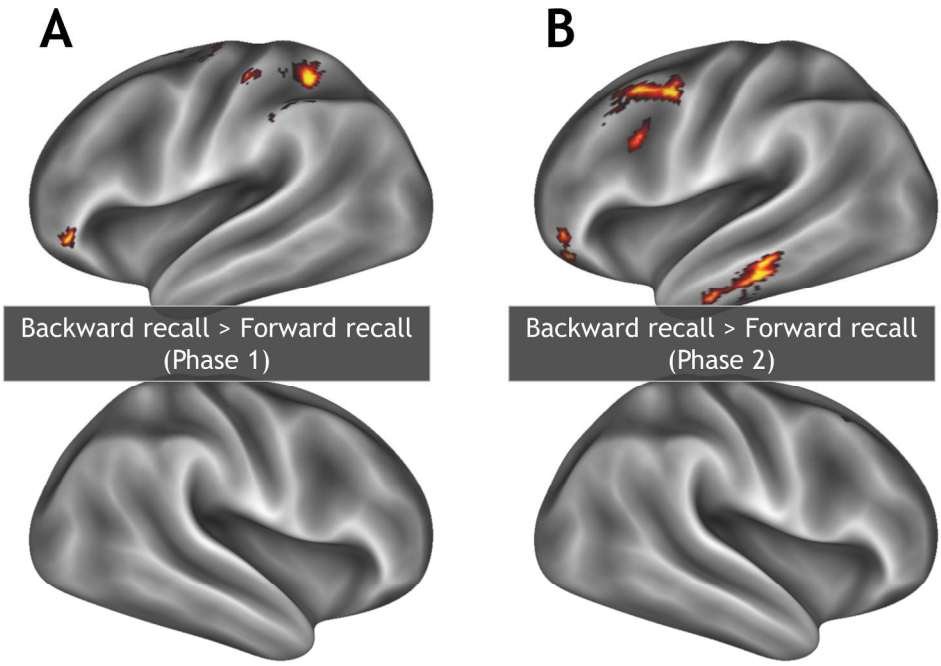

Figure 4. General linear model analysis results. (A) Contrast results for backward versus forward recall conditions in Phase 1. (B) Results from identical contrasts (backward > forward recall conditions) in Phase 2.

239x165mm (300 x 300 DPI)

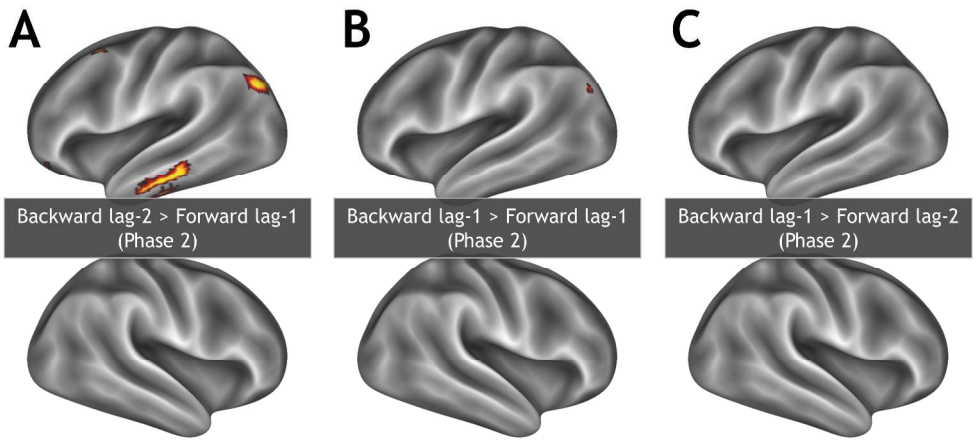

Figure 5. General linear model analysis results of different lag distances. Contrast results for backward versus forward recall conditions with different lag distances in Phase 2. (A) Backward lag-2 > forward lag-1. (B) Backward lag-1 > forward lag-1. (C) Backward lag-1 > forward lag-2.

248x114mm (300 x 300 DPI)

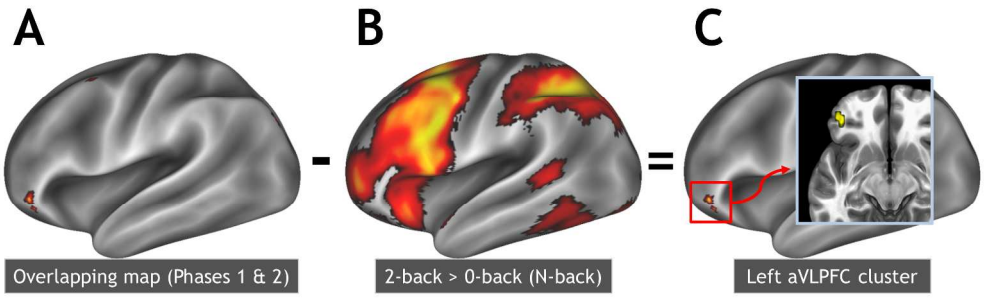

Figure 6. Brain regions commonly recruited across the phases. (A) Overlapping activation map based on the backward versus forward recall results (threshold, $p < .005$) from Phases 1 and 2. (B) Contrast results (threshold, $p < .005$) of 2-back versus 0-back conditions on the N-back task. (C) Subtracting contrast results of the N-back working memory from the overlapping activation map (i.e., A–B) yielded a single cluster ROI in the left anterior ventrolateral prefrontal cortex (aVLPFC).

254x81mm (300 x 300 DPI)

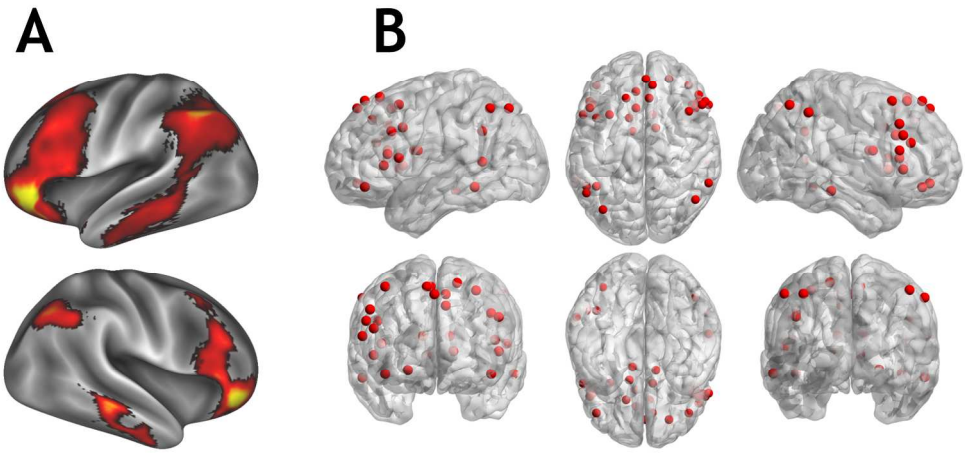

Figure 7. Seed-based resting-state analysis results. (A) Seed-based resting-state analysis, with the left anterior ventrolateral prefrontal cortex (aVLPFC) cluster as the seed region. (B) A total of 35 nodes (shown in red dots) obtained from the seed-based resting-state analysis. Each cube-shaped node was composed of 27 voxels centered on each peak voxel. Plotted nodes are spherical for visualization purposes. From top left in a clockwise direction: sagittal (left lateral), axial (top), sagittal (right lateral), coronal (back), axial (bottom), and coronal (front) views.

211x101mm (300 x 300 DPI)

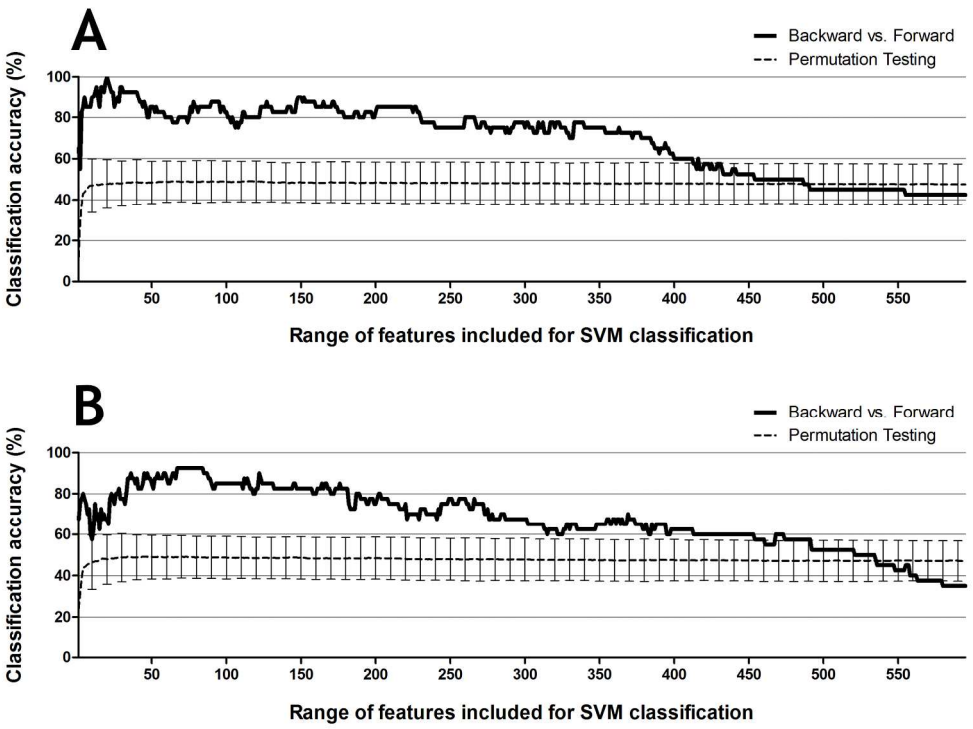

Figure 8. Classification results for functional connectivity multivariate pattern analysis. The thick black lines represent the discrimination accuracies of the support vector machine (SVM) classifier (backward vs. forward retrieval) as a function of the range of features included. Peak accuracies of 100% (Phase 1, A) and 93% (Phase 2, B) were obtained when 20 and 67 features were included in the classification, respectively. The thin black dashed line represents the results of permutation testing, and error bars indicate standard deviation.

223x165mm (300 x 300 DPI)

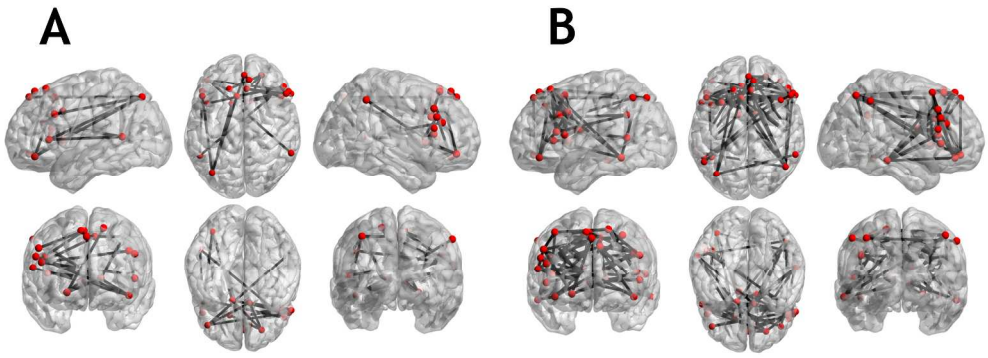

Figure 9. Visualization of included features (edges between the two nodes shown in black lines) and nodes (shown in red dots) at the peak accuracies (100% and 93%, Phases 1 and 2, respectively). A total of 20 features and 21 nodes from Phase 1 (A) and 67 features and 35 nodes from Phase 2 (B) are plotted on the brain template. From top left in a clockwise direction for both panels: sagittal (left lateral), axial (top), sagittal (right lateral), coronal (back), axial (bottom), and coronal (front) views.

254x94mm (300 x 300 DPI)

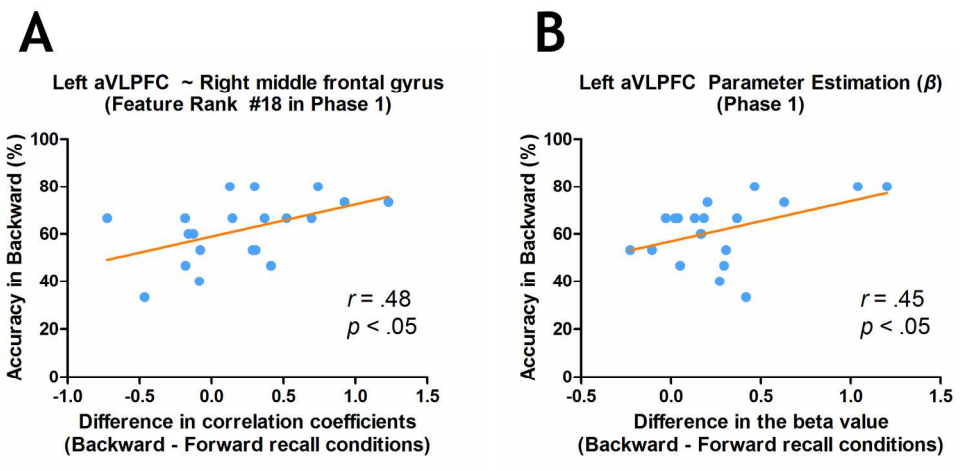

Figure 10. Results of the correlation analysis. (A) The difference in correlation coefficients of the Feature rank #18 (link between the left anterior ventrolateral prefrontal cortex (aVLPFC)–right middle frontal gyrus #3) between two recall conditions (backward recall minus forward recall) was positively correlated with accuracy (%) in the backward condition in Phase 1. (B) A significant positive correlation was observed between the difference in mean parameter estimate for the left aVLPFC (beta values of backward recall minus that of forward recall conditions) and accuracy (%) in the backward condition in Phase 1.

230x109mm (300 x 300 DPI)